CLNS 94/1315
CLEO 94-26
December 14, 1994

Inclusive Decays of B Mesons to Charmonium

R. Balest,[1] K. Cho,[1] W.T. Ford,[1] D.R. Johnson,[1] K. Lingel,[1] M. Lohner,[1] P. Rankin,[1] J.G. Smith,[1] J.P. Alexander,[2] C. Bebek,[2] K. Berkelman,[2] K. Bloom,[2] T.E. Browder,[2*] D.G. Cassel,[2] H.A. Cho,[2] D.M. Coffman,[2] D.S. Crowcroft,[2] P.S. Drell,[2] D.J. Dumas,[2] R. Ehrlich,[2] P. Gaidarev,[2] M. Garcia-Sciveres,[2] B. Geiser,[2] B. Gittelman,[2] S.W. Gray,[2] D.L. Hartill,[2] B.K. Heltsley,[2] S. Henderson,[2] C.D. Jones,[2] S.L. Jones,[2] J. Kandaswamy,[2] N. Katayama,[2] P.C. Kim,[2] D.L. Kreinick,[2] G.S. Ludwig,[2] J. Masui,[2] J. Mevissen,[2] N.B. Mistry,[2] C.R. Ng,[2] E. Nordberg,[2] J.R. Patterson,[2] D. Peterson,[2] D. Riley,[2] S. Salman,[2] M. Sapper,[2] F. Würthwein,[2] P. Avery,[3] A. Freyberger,[3] J. Rodriguez,[3] S. Yang,[3] J. Yelton,[3] D. Cinabro,[4] T. Liu,[4] M. Saulnier,[4] R. Wilson,[4] H. Yamamoto,[4] T. Bergfeld,[5] B.I. Eisenstein,[5] G. Gollin,[5] B. Ong,[5] M. Palmer,[5] M. Selen,[5] J. J. Thaler,[5] K.W. Edwards,[6] M. Ogg,[6] A. Bellerive,[7] D.I. Britton,[7] E.R.F. Hyatt,[7] D.B. MacFarlane,[7] P.M. Patel,[7] B. Spaan,[7] A.J. Sadoff,[8] R. Ammar,[9] P. Baringer,[9] A. Bean,[9] D. Besson,[9] D. Coppage,[9] N. Copty,[9] R. Davis,[9] N. Hancock,[9] M. Kelly,[9] S. Kotov,[9] I. Kravchenko,[9] N. Kwak,[9] H. Lam,[9] Y. Kubota,[10] M. Lattery,[10] M. Momayezi,[10] J.K. Nelson,[10] S. Patton,[10] R. Poling,[10] V. Savinov,[10] S. Schrenk,[10] R. Wang,[10] M.S. Alam,[11] I.J. Kim,[11] Z. Ling,[11] A.H. Mahmood,[11] J.J. O'Neill,[11] H. Severini,[11] C.R. Sun,[11] F. Wappler,[11] G. Crawford,[12] C. M. Daubenmier,[12] R. Fulton,[12] D. Fujino,[12] K.K. Gan,[12] K. Honscheid,[12] H. Kagan,[12] R. Kass,[12] J. Lee,[12] M. Sung,[12] C. White,[12] A. Wolf,[12] M.M. Zoeller,[12] F. Butler,[13] X. Fu,[13] B. Nemati,[13] W.R. Ross,[13] P. Skubic,[13] M. Wood,[13] M. Bishai,[14] J. Fast,[14] E. Gerndt,[14] J.W. Hinson,[14] R.L. McIlwain,[14] T. Miao,[14] D.H. Miller,[14] M. Modesitt,[14] D. Payne,[14] E.I. Shibata,[14] I.P.J. Shipsey,[14] P.N. Wang,[14] M. Battle,[15] J. Ernst,[15] L. Gibbons,[15] Y. Kwon,[15] S. Roberts,[15] E.H. Thorndike,[15] C.H. Wang,[15] J. Dominick,[16] M. Lambrecht,[16] S. Sanghera,[16] V. Shelkov,[16] T. Skwarnicki,[16] R. Stroynowski,[16] I. Volobouev,[16] G. Wei,[16] M. Artuso,[17] M. Gao,[17] M. Goldberg,[17] D. He,[17] N. Horwitz,[17] G.C. Moneti,[17] R. Mountain,[17] F. Muheim,[17] Y. Mukhin,[17] S. Playfer,[17] Y. Rozen,[17] S. Stone,[17] X. Xing,[17] G. Zhu,[17] J. Bartelt,[18] S.E. Csorna,[18] Z. Egyed,[18] V. Jain,[18] D. Gibaut,[19] K. Kinoshita,[19] P. Pomianowski,[19] B. Barish,[20] M. Chadha,[20] S. Chan,[20] D.F. Cowen,[20] G. Eigen,[20] J.S. Miller,[20] C. O'Grady,[20] J. Urheim,[20] A.J. Weinstein,[20] M. Athanas,[21] W. Brower,[21] G. Masek,[21] H.P. Paar,[21] J. Gronberg,[22] C.M. Korte,[22] R. Kutschke,[22] S. Menary,[22] R.J. Morrison,[22] S. Nakanishi,[22] H.N. Nelson,[22] T.K. Nelson,[22] C. Qiao,[22] J.D. Richman,[22] A. Ryd,[22] D. Sperka,[22] H. Tajima,[22] and M.S. Witherell[22]

(CLEO Collaboration)

[1] *University of Colorado, Boulder, Colorado 80309-0390*
[2] *Cornell University, Ithaca, New York 14853*
[3] *University of Florida, Gainesville, Florida 32611*
[4] *Harvard University, Cambridge, Massachusetts 02138*
[5] *University of Illinois, Champaign-Urbana, Illinois, 61801*
[6] *Carleton University, Ottawa, Ontario K1S 5B6 and the Institute of Particle Physics, Canada*
[7] *McGill University, Montréal, Québec H3A 2T8 and the Institute of Particle Physics, Canada*
[8] *Ithaca College, Ithaca, New York 14850*
[9] *University of Kansas, Lawrence, Kansas 66045*
[10] *University of Minnesota, Minneapolis, Minnesota 55455*
[11] *State University of New York at Albany, Albany, New York 12222*
[12] *Ohio State University, Columbus, Ohio, 43210*
[13] *University of Oklahoma, Norman, Oklahoma 73019*
[14] *Purdue University, West Lafayette, Indiana 47907*
[15] *University of Rochester, Rochester, New York 14627*
[16] *Southern Methodist University, Dallas, Texas 75275*
[17] *Syracuse University, Syracuse, New York 13244*
[18] *Vanderbilt University, Nashville, Tennessee 37235*
[19] *Virginia Polytechnic Institute and State University, Blacksburg, Virginia, 24061*
[20] *California Institute of Technology, Pasadena, California 91125*
[21] *University of California, San Diego, La Jolla, California 92093*
[22] *University of California, Santa Barbara, California 93106*
(December 14, 1994)

Abstract

We have used the CLEO-II detector at the Cornell Electron Storage Ring (CESR) to study the inclusive production of charmonium mesons in a sample of 2.15 million $B\overline{B}$ events. We find inclusive branching fractions of $(1.12\pm0.04\pm0.06)\%$ for $B\rightarrow J/\psi$X, $(0.34\pm0.04\pm0.03)\%$ for $B\rightarrow\psi'$X, and $(0.40\pm0.06\pm0.04)\%$ for $B\rightarrow\chi_{c1}$X. We also find some evidence for the inclusive production of χ_{c2}, and set an upper limit for the branching fraction of the inclusive decay $B\rightarrow\eta_c$X of 0.9% at 90% confidence level. Momentum spectra for inclusive J/ψ, ψ' and χ_{c1} production are presented. These measurements are compared to theoretical calculations.

PACS numbers: 13.25.Hw, 14.40.Nd

Typeset using REVTEX

---

*Permanent address: University of Hawaii at Manoa

I. INTRODUCTION

Inclusive decays of B mesons to charmonium states provide a testing ground for QCD calculations of quark dynamics. The basic decay mechanism for B mesons is the spectator diagram shown in Fig. 1a. The dominant mechanism for production of charmonium, however, is the color-suppressed internal spectator diagram, shown in Fig. 1b. Virtual gluon interactions complicate this picture, leading to an "effective neutral current" [1,2]. These gluon interactions are difficult to handle in QCD, and alternative approaches to these calculations [3,4] can result in significantly different predictions. Precise measurements of the inclusive branching fractions for B-meson decays to different charmonium states provide sensitive tests of these models. Measurements of B decays to charmonium are also important ingredients in the study of b-quark production in hadronic interactions [5–7]. There has been particular interest in the momentum spectra for charmonium production in B decays.

Both ARGUS and CLEO have reported previously on B decays to charmonium [8–13]. In this paper we report on the inclusive decays of B mesons to J/ψ, ψ', χ_c and η_c, where the "B" represents the mixture of B^0 and B^+ in $\Upsilon(4S)$ decays. (This mixture is expected to be roughly equal, based on the very small mass difference between the two mesons.) Our B-meson data sample is approximately ten times larger than those of previous studies. Our results represent significant improvements in precision for all modes investigated. The inclusive studies reported here are complementary to CLEO-II measurements of exclusive B decays to charmonium which have recently been reported [14,15].

II. DATA SAMPLE AND EVENT SELECTION

The data used in this analysis were recorded with the CLEO-II detector, located at the Cornell Electron Storage Ring (CESR). An integrated luminosity of 2.02 fb^{-1} was accumulated at the $\Upsilon(4S)$ resonance, and an additional 0.99 fb^{-1} was collected at energies just below the threshold for $B\overline{B}$ production. Because the $B \to J/\psi$ inclusive measurement is systematics limited, only the data for which the systematic uncertainties are best understood were used to study that decay mode (1.12 fb^{-1} taken at the $\Upsilon(4S)$ resonance and 0.53 fb^{-1} at energies just below).

The CLEO-II detector [16] consists of three concentric cylindrical wire drift chambers surrounded by a time-of-flight system and an electromagnetic calorimeter of 7800 thallium-doped cesium iodide crystals. Surrounding the calorimeter is a 1.5-Tesla superconducting solenoidal magnet. Outside the magnet are three layers of steel interleaved with muon detection chambers. In the barrel region of the detector (defined as the region where the angle of the shower or track with respect to the beam axis lies between 45° and 135°), the rms shower energy resolution is given by $\delta E/E = (0.35/E^{0.75} + 1.9 - 0.1E)\%$, where E is in GeV. For photons in the energy range that is most important for this study, the resolution is about 2.5%. The charged particle momentum resolution is given by $(\delta p_t/p_t)^2 = (0.0015p_t)^2 + (0.005)^2$, where p_t is in GeV/c.

Event-selection criteria were optimized for $\Upsilon(4S)$ events with B or $\overline{B}$ decays to charmonium. Events were required to have a reconstructed vertex consistent with the known interaction region, and to have detected visible energy greater than 15% of the center-of-mass energy. To suppress background from QED processes we required at least five reconstructed charged tracks. While $B\overline{B}$ events tend to be spherical, as B mesons produced in $\Upsilon(4S)$ decays are almost at rest, the background continuum production of light quark pairs tends to produce two jets. Event-shape properties were therefore used to suppress continuum background. We required events to have a second order normalized Fox-Wolfram moment ($R_2 = H_2/H_0$) of less than 0.5 [17]. We found $(2.15\pm0.04)\times10^6$ $B\overline{B}$ events which satisfied these requirements in the full sample, and $(1.19\pm0.02)\times10^6$ in the smaller sample used to study $B\to J/\psi$X.

III. SELECTION OF J/ψ AND ψ' CANDIDATES

The charmonium mesons J/ψ and ψ' were reconstructed through their decays to e^+e^- and $\mu^+\mu^-$. We also reconstructed ψ' through its decay to $J/\psi\,\pi^+\pi^-$. The χ_c states were reconstructed though their radiative decays to J/ψ. The small B-meson momentum at the $\Upsilon(4S)$ provides constraints on the kinematics of decays to charmonium which we exploited to suppress continuum and combinatorial backgrounds. The J/ψ and ψ' candidates were required to have momenta less than 2.0 GeV/c and 1.65 GeV/c, respectively. These cuts were chosen to be slightly higher than the maximum momenta for the Cabibbo-suppressed decay modes $B\to J/\psi(\psi')\pi$. Because of the large amount of energy in the leptonic decay of the J/ψ and ψ', low energy leptons cannot be produced, and we imposed a minimum lepton momentum requirement of 0.8 GeV/c in searching for charmonium candidates.

To identify electrons, information from several detector components was combined. The energy deposited in the electromagnetic calorimeter had to be consistent with the measured track momentum, and the specific ionization (dE/dx) in the main drift chamber had to be consistent with that expected for an electron. For dielectron J/ψ candidates, both electrons were required to project into the barrel region of the calorimeter ($|\cos\theta| < 0.7$, where θ is the polar angle). For ψ' and χ_c events, we allowed one electron to project into the expanded angular range $|\cos\theta| < 0.91$. The tighter requirement for J/ψ candidates was chosen because the efficiency for identifying electrons is better known in the barrel part of the calorimeter than at the ends. The efficiency for detecting and identifying electrons in this region is about 90%, and the probability for a hadron to be misidentified as an electron is approximately 0.3%.

Muons were identified by matching charged tracks to hits in proportional tubes embedded in the steel hadron absorber. At least one of the muons was required to have penetrated five nuclear interaction lengths, while the other was required to have penetrated three. The efficiency for detecting 2.5 GeV/c muons that have passed through five interaction lengths of material in the barrel region is 94%. At this depth the probability for a hadron to be misidentified as a muon is approximately 1%.

IV. $B\to J/\psi$X

The invariant mass distributions for dielectrons and dimuons in our 1.12 fb^{-1} $\Upsilon(4S)$ data sample are shown in Fig. 2. The background functions for both fits are second-order polynomials. The J/ψ signals were fitted to histograms derived from a Monte Carlo simulation of

$B \to J/\psi X$, $J/\psi \to e^+e^-$ or $\mu^+\mu^-$. Since the detection efficiency is potentially sensitive to the J/ψ momentum, these Monte Carlo events were generated using an iterative procedure to approximate the observed momentum spectrum in data. This simulation included the effects of bremsstrahlung in the detector material and of final state electromagnetic radiation in the J/ψ decay [18]. Fig. 3 shows the dielectron and dimuon mass distributions, generated with and without final-state radiation. Approximately 6% of the detected dimuon and 35% of the detected dielectron J/ψ's have masses between 2.50 and 3.05 GeV/c^2, more than 3σ below the J/ψ mass.

The results of the fits to the dilepton mass distributions in Fig. 2 are signals for $B \to J/\psi X$ of 741$\pm$37 events in the dielectron mode, and 748$\pm$32 events in the dimuon mode, where the errors are statistical only. The background contribution to the mass peak from continuum J/ψ production was determined using the data collected below the $\Upsilon(4S)$ resonance. As has been previously reported [12], there is continuum production of J/ψ mesons, but it is only evident for dilepton momenta above 2.0 GeV/c. Fig. 4 shows the dilepton mass spectra for the 0.53 fb^{-1} below-resonance data sample. The minimum momentum requirement of 2.0 GeV/c and the continuum-suppressing cut $R_2 < 0.5$ have been imposed. Fits to the distributions in Fig. 4 give statistically insignificant excesses of 8.8$\pm$5.3 dielectrons and 7.3$\pm$5.0 dimuons. To determine the continuum subtractions which must be applied to our $\Upsilon(4S)$ signals, these yields must be scaled by 2.12$\pm$0.01, which is the ratio of the integrated luminosities of the samples after correction for the energy dependence of the continuum cross section. The resulting corrections are 18.7$\pm$11.3 dielectrons and 15.4$\pm$10.5 dimuons. Details of continuum J/ψ production will be presented in a forthcoming publication.

The efficiencies for detecting dielectron and dimuon J/ψ decays with dilepton masses between 2.5 and 3.5 GeV/c^2 were determined from the Monte Carlo simulation to be (45.3$\pm$0.4)% and (46.4$\pm$0.4)%, where the errors are due to the statistics of the Monte Carlo sample. The detection efficiencies are shown as a function of J/ψ momentum in Fig. 5. For dimuons the efficiency is constant over the momentum range of interest, while for electrons the efficiency decreases with increasing J/ψ momentum as a result of limiting the electrons to the barrel region of the detector. Slowly moving J/ψ's that decay leptonically produce nearly back-to-back lepton pairs, so if one lepton passes through the barrel region, the other is also likely to do so. Leptons from a fast moving J/ψ will be boosted in the direction of the J/ψ, so if one lepton passes through the barrel the other may not. The efficiency for detecting dielectron J/ψ's is independent of momentum when one electron is allowed to be in the end-cap region of the detector. The systematic error introduced by the change in efficiency over the momentum region of interest and the uncertainty in matching the Monte Carlo and data spectra is 2% for the dielectrons and much smaller than 1% for the dimuons.

Using values for the branching ratios for J/ψ decays to dielectrons and dimuons of (5.99$\pm$0.25)% and (5.97$\pm$0.25)%, respectively [19], we find the branching fraction for $B \to J/\psi X$ to be (1.12$\pm$0.06)% using the dielectron yield, and (1.12$\pm$0.05)% using the dimuon yield. The given errors are statistical only. Systematic uncertainties dominate the overall error in the inclusive J/ψ measurement. Significant uncertainties are associated with the lepton-identification efficiencies and the J/ψ to dilepton branching fractions. The first of these errors enters twice, once for each lepton. Other smaller errors include those associated with Monte Carlo statistics, the Monte Carlo J/ψ momentum distribution (through the momentum-dependent efficiency), the Monte Carlo line shape used in the fit, the tracking efficiency, the number of B mesons in the data sample, and the efficiency of the requirement $R_2 < 0.5$. A summary of the systematic errors is given in Table I.

The $B \to J/\psi X$ branching fractions measured with dimuon and dielectron events were combined with weights determined from the statistical and uncorrelated systematic errors. The combined branching fraction for $B \to J/\psi X$ is $(1.12 \pm 0.04 \pm 0.06)\%$, where the first error is statistical and the second systematic. This can be compared to the previous world average as compiled by the Particle Data Group (PDG), $(1.30 \pm 0.17)\%$ [19]. The new result is a large improvement in precision over the previous world average.

The inclusive $B \to \psi' X$ and $B \to \chi_c X$ branching fractions were measured with the full 2.02 fb^{-1} $\Upsilon(4S)$ data set. The additional 0.90 fb^{-1} has not been studied as intensively as the 1.12 fb^{-1} used for the J/ψ measurement. To establish that differences in efficiencies and other systematic effects are not significant, we have compared the inclusive J/ψ yields. They agree to within one standard deviation of the statistical error. On this basis we are confident of the reliability of the full data sample for the statistics-limited studies of decays to charmonium states other than J/ψ.

V. $B \to \psi' X$

We have measured B-meson decays to ψ' using two decay channels. The analysis based on the dilepton decay $\psi' \to \ell^+\ell^-$ is very similar to the J/ψ study, but is hampered by a much smaller leptonic branching fraction. A second analysis, based on the hadronic transition $\psi' \to J/\psi \pi^+\pi^-$ followed by the leptonic decay of J/ψ, provides an independent measurement with different systematic considerations. In the following sections we describe these measurements separately, and conclude with a brief description of how they have been combined.

A. $\psi' \to \ell^+\ell^-$

The distributions of dielectron and dimuon invariant masses in the ψ' region are shown in Fig. 6, both separately and combined. We determined the ψ' yield by fitting the distributions with Monte Carlo signal shapes and polynomial backgrounds. We found signals of 68 ± 17 dielectrons and 59 ± 13 dimuons, where the errors are statistical only. The efficiency for detecting the ψ' is 59% in both the dielectron and dimuon modes, significantly higher than the corresponding efficiencies for J/ψ. The higher dielectron efficiency results from using the end-cap region of the calorimeter. The higher dimuon efficiency is a consequence of the greater momentum of muons from ψ' decay, which allows a larger fraction to penetrate the iron absorber.

Using the Particle Data Group [19] branching fractions for $\psi' \to e^+e^-$ and $\psi' \to \mu^+\mu^-$ of $(0.88 \pm 0.13)\%$ and $(0.77 \pm 0.17)\%$, respectively, we find branching fractions for $B \to \psi' X$ of $(0.31 \pm 0.08)\%$ and $(0.30 \pm 0.07)\%$. The sources of systematic uncertainty are the same as for the J/ψ, except that the error in the leptonic branching fraction is much larger than for the J/ψ (15% for $\psi' \to e^+e^-$ and 22% for $\psi' \to \mu^+\mu^-$), and is dominant. The error in the efficiency for identifying both electrons increases from 4% to 6% as a result of using the end-cap region of the detector. We have combined the two modes with weights given by the statistical and uncorrelated systematic errors. The resulting branching fraction for $B \to \psi' X$ is $(0.30 \pm 0.05 \pm 0.04)\%$.

B. $\psi' \to J/\psi \pi^+ \pi^-$

A second, statistically independent, measurement of the $B \to \psi' X$ branching fraction has been made using the decay chain $\psi' \to J/\psi \pi^+ \pi^-$, $J/\psi \to \ell^+ \ell^-$. The product branching fraction for this process (32.4% for $\psi' \to J/\psi \pi^+ \pi^-$, 12.0% for $J/\psi \to \ell^+ \ell^-$ [19]) is roughly a factor of 2 greater than the $\psi' \to \ell^+ \ell^-$ branching fraction. This advantage is diminished by the inefficiencies associated with reconstructing the two charged pions. The overall efficiency for detecting ψ' mesons in this channel is comparable to that of the dilepton measurement.

To search for ψ' decays in this mode we first selected events where the J/ψ candidates had an invariant mass within two standard deviations (σ = 15 MeV) of the measured J/ψ mass. The width of the J/ψ was determined by fitting the data to the Crystal Ball function [20], which provides an adequate description of the radiative tail. The efficiency for J/ψ's to satisfy the mass criterion (including tracking and lepton identification) is 35% for dielectrons and 41% for dimuons. Note that we allowed the second electron in the J/ψ candidate to be outside the barrel region of the detector.

Pion candidates were required to have specific ionization within three standard deviations of the expected value. Tracks that were identified as daughters of a K_S^0 were vetoed. It has been shown that the $\pi^+ \pi^-$ invariant mass spectrum from ψ' decays favors larger values than would be expected from phase space (Fig. 7) [21]. We required the invariant mass of the dipion system to be between 0.45 and 0.58 GeV/c^2. This cut has an efficiency of $(86 \pm 5)\%$, while rejecting over half of all random dipions.

In Fig. 8 we present the distributions of the difference between the masses of reconstructed ψ' and J/ψ candidates for dielectrons, dimuons and both combined. Using the mass difference reduces the effect of the error in the J/ψ mass measurement. The data were fitted to a second order polynomial with a Monte Carlo signal shape. We found signals of 48 ± 10 in the dielectron channel and 65 ± 12 in the dimuon channel, where the errors are statistical only. The efficiency for finding $\psi' \to J/\psi \pi^+ \pi^-$ in the dielectron mode is 17%, while for the dimuon mode it is 20%. We find branching fractions for $B \to \psi' X$ of $(0.35 \pm 0.07)\%$ for the dielectron mode and $(0.39 \pm 0.07)\%$ for the dimuon mode. The sources of systematic uncertainty include those for the $B \to J/\psi X$ measurement as well as a 2% error in the efficiency for finding each pion track, a 2% error in the efficiency for identification for each pion, a 6% error in the efficiency of the dipion mass requirement, and an 8% error in the $\psi' \to J/\psi \pi^+ \pi^-$ branching fraction. For the dielectron mode, the error in the efficiency for identifying both leptons is 6%, since we include the end-cap region of the detector.

The dielectron and dimuon modes have been combined, weighted by the statistical and uncorrelated systematic errors, to give a B to ψ' inclusive branching fraction of $(0.37 \pm 0.05 \pm 0.05)\%$.

C. Combining the Two $B \to \psi' X$ Modes

Our two measurements of the branching fraction for $B \to \psi' X$ are in good agreement. Since the samples are statistically independent they can be combined into a single result. Using relative weights determined from the statistical and uncorrelated systematic errors, we find the branching fraction for $B \to \psi' X$ to be $(0.34 \pm 0.04 \pm 0.03)\%$.

VI. $B \to \chi_C X$

Inclusive χ_c events were reconstructed by combining photons detected in the cesium iodide calorimeter with any accompanying J/ψ candidates. The observed distribution of the mass difference between the χ_c and J/ψ candidates was fitted to the the expectation for the decay chain $B \to \chi_c X$, $\chi_c \to J/\psi \gamma$, $J/\psi \to \ell^+ \ell^-$. We demanded the mass of the J/ψ candidate for the χ_c search to be within two standard deviations of the nominal J/ψ mass, as was done for the $\psi' \to J/\psi \pi^+ \pi^-$ search.

A. Selection of Photon Candidates

We selected photon candidates from showers in the cesium iodide calorimeter with energies of at least 75 MeV. We rejected showers that were matched to charged tracks or were in the region of the end-cap calorimeter with inferior resolution.

The largest background to the χ_c signal is due to random combinations of photons from π^0's with correctly reconstructed J/ψ's from B-meson decays. Monte Carlo studies showed that the statistical significance of the $B \to \chi_c X$ measurement is optimized by imposing stringent π^0-suppression requirements. Therefore any candidate photon which could be combined with another photon to produce an effective mass near the π^0 mass was rejected. The Monte Carlo studies revealed that signal photons were occasionally vetoed when they were combined with a low-energy photon from an uncorrelated π^0. The reduction of this effect was the primary motivation for the 75 MeV energy cut. If the invariant mass of a photon pair was within a range of -5 to 3 standard deviations of the measured π^0 mass, the photons were flagged as being part of a π^0 and were not used. The width of the π^0 peak was determined by fitting the diphoton mass plot (Fig. 9) for different momentum intervals with the Crystal Ball function [20]. This function adequately parameterizes the long tail on the lower side, which results from photon energy leaking out of the crystals and the shower energy being underestimated.

Further selection criteria were imposed on the remaining showers. We required showers to be in the barrel region of the calorimeter ($|\cos\theta| < 0.7$), and to have a shape consistent with that expected for a photon. Finally, we rejected showers that were within 9° of the intersection of a charged track with the crystals, eliminating the debris from charged particle interactions.

Monte Carlo studies showed that the remaining background consists predominantly of photons from unsuppressed π^0's (73%), and photons from η decays (18%).

B. Fitting the Mass Difference

Since the background to the χ_c signal comes mostly from real J/ψ's combined with uncorrelated photons, a Monte Carlo simulation should model the background well. We verified this expectation by making various combinations of Monte Carlo and data photons with Monte Carlo and data J/ψ candidates. The magnitude of the background is simulated to within one standard deviation by the J/ψ Monte Carlo, if one scales the Monte Carlo prediction to the observed number of J/ψ candidates plus the random dilepton background within the J/ψ mass window.

Fig. 10 shows a fit with only the χ_{c1} allowed. The χ_{c1} line shape was determined with Monte Carlo. In this case we find 112$\pm$17 events. A better fit is obtained by allowing for both the χ_{c1} and χ_{c2} (Fig. 11), with the mass difference between the χ_{c1} and χ_{c2} fixed in the fit to the previously measured value of (45.6 ± 0.2) MeV [19]. We find the χ_{c1} signal to be unchanged, 112$\pm$17 events, and also find 35$\pm$13 events in the χ_{c2} region. To help investigate the sensitivity of the result to the functional form used to fit the background, we also fitted with a second order Chebychev polynomial. In this case, the number of events in the χ_{c1} peak is 110$\pm$18, and the excess in the χ_{c2} region is 37$\pm$14.

The world average branching fractions for $\chi_{c1}\rightarrow J/\psi\gamma$ and $\chi_{c2}\rightarrow J/\psi\gamma$ are (27.3$\pm$1.6)% and (13.5$\pm$1.1)%, respectively [19]. We would not expect to see χ_{c0} even if it were produced, because the branching fraction for $\chi_{c0}\rightarrow J/\psi\gamma$ is only (0.66$\pm$0.18)%. The efficiencies for detecting χ_{c1} and χ_{c2} were both determined from Monte Carlo to be 20%. We use the numbers from the fit with the Monte Carlo background shape to determine the branching fraction, and use the alternative fit with the polynomial background to help assess the systematic error. The branching fraction for $B\rightarrow\chi_{c1}$X is (0.40$\pm$0.06$\pm$0.04)%. The dominant systematic errors are associated with identifying the leptons and with the $\chi_{c1}\rightarrow J/\psi\gamma$ branching fraction. The systematic error in the efficiency for identifying the photon is 2.5%. The upper limit for the $B\rightarrow\chi_{c2}$X branching fraction is 0.38% at 90% confidence level. If we interpret the excess in the χ_{c2} signal region of the mass difference plot as $B\rightarrow\chi_{c2}$X, we find a branching fraction of (0.25$\pm$0.10$\pm$0.03)%.

VII. MOMENTUM SPECTRUM OF J/ψ, ψ' AND χ_{C1} FROM B DECAY

The momentum spectrum of the inclusive J/ψ's was measured by dividing the candidate sample into momentum bins of 100 MeV/c between 0 and 2 GeV/c. Each of the resulting dielectron and dimuon mass distributions was fitted to determine the J/ψ yield in that bin, which was then corrected for that bin's efficiency. The resulting momentum distribution is shown in Fig. 12.

In Fig. 13 the J/ψ momentum spectrum is again shown, this time overlaid with the expected contributions from the exclusive modes $B\rightarrow J/\psi K$ and $B\rightarrow J/\psi K^*$ [14], and from the feed-down modes $B\rightarrow\chi_c$X, $\chi_c\rightarrow J/\psi\gamma$ and $B\rightarrow\psi'$X, $\psi'\rightarrow J/\psi\pi^+\pi^-$. Each contribution is normalized to the corresponding CLEO-II measured branching fraction. The momentum spectra for the feed-down modes are from Monte Carlo simulations. The sum of the known contributions is also shown. The difference between this sum and the measured momentum spectrum of the J/ψ's suggests a sizable contribution from higher K^* resonances or nonresonant multiparticle final states.

For comparison with theory it is more interesting to measure the momentum spectra for direct production of charmonium in B decays. Shown in Fig. 14 is the J/ψ momentum spectrum with the expected contributions from the feed-down modes $B \to \psi' X$ and $B \to \chi_c X$ subtracted. We have also measured the momentum distribution of inclusively produced ψ''s, which are all believed to be directly produced. In this case, the momentum spectrum for each of the two ψ' decay modes was obtained by separately fitting the data in 200 MeV/c momentum bins. The momentum spectra for the two modes were combined with the same weights as were used to combine the two branching fractions. The resulting inclusive ψ' spectrum is shown in Fig. 15. The momentum distribution for χ_{c1} was similarly determined by subdividing the $J/\psi\gamma$ sample into momentum bins which were fitted separately. The resulting spectrum, which is shown in Fig. 16, is not as well measured, but appears to be quite similar to the J/ψ and ψ' momentum spectra. In all cases there is significant low-momentum charmonium production, suggesting a sizable component of decays with with three or more particles in the final state.

VIII. $B \to \eta_C X$

We have also searched for the decay $B \to \eta_c X$. The η_c is more difficult to detect than the J/ψ meson as it lacks a single decay channel with both a sizable branching ratio and manageable backgrounds. We searched for the decay $\eta_c \to \phi\phi$ with $\phi \to K^+K^-$. This channel has enough distinctive features to allow for efficient suppression of background, but has a branching fraction of only $(0.71 \pm 0.28)\%$ [19].

All four kaon tracks were required to be well measured and to originate from the interaction point. To select pairs of kaons, with good suppression of the more abundant pions, we computed a combined likelihood using the dE/dx and time-of-flight measurements for both tracks forming a ϕ candidate. We required the kaon likelihood of the tracks to be greater than 5%. The invariant masses of both ϕ candidates were combined into a χ^2 using the measured mass and resolution (2.7 MeV rms) for ϕ mesons. Combinations with $\chi^2 > 10$ were rejected.

We searched for the signal in the invariant mass distribution of the two ϕ's. The η_c mass resolution was determined by Monte Carlo simulation to be 7 MeV. (The η_c natural width is $10^{+3.8}_{-3.4}$ MeV [19].) A new measurement of the η_c mass from E760 (m_{η_c}=2989.9$\pm$2.2$\pm$0.4 MeV) [22] is significantly higher than the value compiled by the PDG (m_{η_c}=2978.8$\pm$1.9 MeV). We define the signal region to be the interval 2960 to 3010 MeV, which accommodates the uncertainty in the η_c mass. For each η_c candidate, we imposed a maximum momentum requirement of 2 GeV/c, which is the largest momentum allowed for η_c mesons produced in B-meson decays. To suppress backgrounds from continuum production of ϕ-meson pairs we required $R_2 < 0.3$ [17]. Additional suppression of background was achieved by a spin-parity analysis using the distribution of the angle χ between the two ϕ decay planes in the $\phi\phi$ rest frame. For the pseudoscalar η_c decaying into two vector mesons the χ distribution is proportional to $1 - \cos(2\chi)$ [23]. Our requirement of $\chi > 45°$ is 82% efficient for signal and reduces the background, expected to be flat, by a factor of two.

We show the result in Fig. 17a, where we plot the invariant mass distribution of the final $\phi\phi$ sample. There are 8 candidate events in the signal region. The background in this region is mainly due to random combinations when both B mesons in the event produce a ϕ. The number of background events in the signal region was estimated by fitting the $\phi\phi$ mass distribution with different functions (first and second order Chebychev polynomials and exponentials) with the signal region excluded. As a check we also fitted the $\chi < 45°$ sample. We estimate 7.2±1.0 background events in the signal region. Using the prescription of the PDG [19] for the case of Poisson processes with background we obtain an upper limit of less than 6.6 signal events at 90% confidence level. In Fig. 17b we show the expected signal distribution from a Monte Carlo simulation. From this distribution we determine the efficiency for detecting the η_c to be 15.5%.

The systematic error on the signal efficiency consists of a 2% error in the efficiency for finding each kaon track; an 11.5% error from the kaon identification, which has been determined using data; a 5% error accounting for possible variations in the η_c momentum spectrum (we assumed a shape similar to the J/ψ momentum spectrum); and a 4.5% error from Monte Carlo statistics. The error in the number of background events in the signal region contributes a 10% uncertainty in the upper limit and is included in the total systematic error. The total systematic error, however, is dominated by the 40% uncertainty in the branching fraction $\mathcal{B}(\eta_c \to \phi\phi)$.

Using the intermediate branching fractions for $\eta_c \to \phi\phi$ (0.71±0.28)% and for $\phi \to K^+K^-$ (49.1±0.8)%, as well as the signal efficiency and the number of B mesons in our data sample, we derive an upper limit on the branching ratio $\mathcal{B}(B \to \eta_c \mathrm{X})$ of 0.9 % at 90% confidence level. The total relative systematic error of 44% has been incorporated by increasing the upper limit by 1.28 times the error itself.

IX. SUMMARY OF EXPERIMENTAL RESULTS

Table II summarizes our inclusive measurements and, for comparison, presents the corresponding values compiled by the Particle Data Group (PDG) [19]. Our result for the $B \to J/\psi\mathrm{X}$ branching fraction is consistent with the previous determination, and the error has been reduced by a factor of 2.4. The new measurement for the branching fraction for $B \to \psi'\mathrm{X}$ is also consistent with the PDG value, and in this case the precision has been improved by a factor of 4.

ARGUS has reported a $B \to \chi_{c1}\mathrm{X}$ branching fraction of (1.05±0.35±0.25)% [13]. Their study did not have sufficient energy resolution to distinguish a χ_{c1} signal from possible χ_{c2} production. On theoretical grounds they assumed that their signal was entirely $B \to \chi_{c1}\mathrm{X}$. The new CLEO-II measurement is 1.5 standard deviations lower than the ARGUS measurement. It is 2.2 standard deviations lower than the L3 measurement of (2.4±0.9±0.2)% [24]. It is consistent with a preliminary CLEO-II measurement (0.54±0.15±0.09)% [12], which was based on the first 30% of the data sample used for this analysis. The χ_{c2} measurement is 2.5 standard deviations in statistical significance.

The measured branching fraction for $B \to J/\psi\mathrm{X}$ is composed of two parts: "direct" production, and "feed down" from charmonium modes, such as $B \to \psi'\mathrm{X}$, $\psi' \to J/\psi\pi^+\pi^-$. To obtain the direct rate for comparison with theoretical predictions, we need to correct the inclusive branching fraction for the feed-down component. Assuming that all the feed down comes from ψ' and χ_c, we find the direct branching fraction to be $(0.80\pm0.08)\%$ (Table III). The $B\to\chi_{c1}$X branching fraction must also be adjusted slightly for feed down from ψ''s. We assume that the direct branching fraction for $B\to\psi'$X is equal to the measured branching fraction since there is no known feed-down mechanism for ψ' production. (Charmonium states with masses above the ψ' are above the threshold for $D\overline{D}$ meson production and decay almost exclusively through that mode.)

The upper limit on the branching fraction for $B\to\eta_c$X of 0.9% (90% confidence level) is the first search for B to charmonium decays using a decay mode with neither a J/ψ or ψ'.

X. COMPARISON WITH THEORETICAL PREDICTIONS

The basic interaction Hamiltonian for charmonium production in B-meson decay is

$$H_{Weak} = \frac{G_F}{\sqrt{2}} V_{cb} V_{cs}^* (\overline{s}c)(\overline{c}b). \tag{1}$$

For the decay of B mesons to charmonium states, the $\overline{c}$ from the W must combine with the c from the b (Fig. 1b). For this internal spectator diagram, the c-quark color must match the $\overline{c}$-quark color to form a color singlet meson state. Naively, the requirement of color matching introduces a factor of one third in the amplitude for the internal spectator decay. This leads to a predicted rate for the B-meson decay to charmonium which is one ninth of that expected without accounting for color [3,25].

Virtual gluon interactions can take place between the quarks, leading to additional Feynman diagrams. The virtual gluons can "rearrange" the final state quarks, swapping the c created when the b decays with the s produced in the W^- decay. The gluon interactions lead to an additional term in the interaction Hamiltonian with the quark pairings $(\overline{s}b)$ and $(\overline{c}c)$:

$$H_{Effective} = \frac{G_F}{\sqrt{2}} V_{cb} V_{cs}^* \left[c_1(\mu)(\overline{s}c)(\overline{c}b) + c_2(\mu)(\overline{c}c)(\overline{s}b)\right]. \tag{2}$$

The "Wilson" coefficients $c_1(\mu)$ and $c_2(\mu)$ which enter the Hamiltonian can be calculated from QCD [26]:

$$c_\pm(\mu) = c_1(\mu) \pm c_2(\mu), \tag{3}$$

$$c_\pm(\mu) = \left(\frac{\alpha_s(M_W^2)}{\alpha_s(\mu)}\right)^{\frac{-6\gamma\pm}{(33-2n_f)}}, \tag{4}$$

where $\gamma_- = -2\gamma_+ = 2$, n_f is the number of contributing quark flavors (expected to be five for B-meson decay), and μ is usually taken to be $\sim m_b^2$.

To find the contribution of the c_1 term to charmonium production one performs a Fierz-transformation:

$$(\overline{c}_a b_a)(\overline{s}_b c_b) = \frac{1}{3}(\overline{s}_a b_a)(\overline{c}_b c_b) + \frac{1}{2}(\overline{s}\lambda_i b)(\overline{c}\lambda_i c), \tag{5}$$

where λ_i are SU(3) color matrices and the subscript explicitly keeps track of the color [3]. The Hamiltonian becomes

$$H_{Effective} = \frac{G_F}{\sqrt{2}} V_{cb} V_{cs}^* \left[\left(\frac{1}{3} c_1(\mu) + c_2(\mu) \right) (\overline{c}c)(\overline{s}b) + \frac{1}{2} c_1(\mu) (\overline{s}\lambda_i b)(\overline{c}\lambda_i c) \right]. \quad (6)$$

The first part of Eq. (6) transforms as a color singlet. From conservation laws this singlet part contributes to the formation of the J/ψ, ψ', χ_{c1} and η_c states. The second part of Eq. (6) transforms as a color octet. As pointed out by Bodwin *et al.*, the octet part can contribute to the formation of χ_{c0}, χ_{c1}, χ_{c2} and h_c states [4]. The $\frac{1}{3}$ in the singlet part reflects color suppression. If the $\frac{1}{3}$ is replaced by $1/N_C$ then the coefficient of the color singlet part is equivalent to the a_2 term in the factorization model of Bauer, Stech and Wirbel for exclusive decays [27]. The difference between $1/N_C$ and $\frac{1}{3}$ parameterizes the non-factorizable contributions to B-meson decay [28].

The difficulty of calculating absolute branching fractions for hadronic decays is demonstrated by the spread of values calculated by theorists following similar recipes. Predicted branching fractions for direct $B{\rightarrow}J/\psi$X range from 0.2% to 2.0%, depending on the value selected for α_s (on which the Wilson coefficients c_1 and c_2 depend) and the magnitude of the color suppression (the $1/N_C$ coefficient) assumed [3,4,25,29,30]. With the number of colors set to three, the contributions of c_1 and c_2 almost cancel in the color-singlet term. Following the method of Ref. [4] and using the values $c_1 = 1.13$ and $c_2 = -0.29$, which include next-to-leading log corrections [28], and a b mass of 5.0 GeV/c^2, we find the prediction for the direct branching fraction for $B{\rightarrow}J/\psi$X to be 0.10%. However, if one replaces $(\frac{1}{3}c_1 + c_2)$ by the measured value of a_2 from exclusive decays (0.23$\pm$0.01$\pm$0.01 [31]) then one predicts the direct branching fraction for $B{\rightarrow}J/\psi$X to be 0.75%, in good agreement with our measured value.

The success of using a_2 in this way prompts us to examine the predictions of Bodwin *et al.* for χ_{c2} production [4]. While χ_{c1} can be produced by both the color-singlet and color-octet mechanisms, χ_{c2} can only be produced via the octet mechanism. The difference in the predicted χ_{c1} branching fraction from the color-singlet term and our measured branching fraction gives a measure of color-octet production. Bodwin *et al.* predict the ratio of χ_{c2} production to χ_{c1} production to be 1.3:1.0. Following their method, but with the values of c_1, c_2 and the b mass given above, and using the branching fraction for χ_{c1} presented here, we find that the ratio should be 1.6:1.0. This leads to a predicted branching fraction for $B{\rightarrow}\chi_{c2}$X of (0.56$\pm$0.15)%, where the error is limited to the experimental error of the inputs. This prediction is somewhat larger than our 90% confidence level upper limit on the $B{\rightarrow}\chi_{c2}$X branching fraction (Table II). They have assumed $N_C = 3$, implying a very small contribution from the color-singlet mode, and therefore that the major contribution to the $B{\rightarrow}\chi_{c1}$X branching fraction is the color-octet mechanism. When we replace $(\frac{1}{3}c_1 + c_2)$ by a_2, the predicted color-singlet contribution to χ_{c1} production is 0.19%, leaving 0.18% for the color-octet contribution. This leads to a prediction for the direct $B{\rightarrow}\chi_{c2}$X branching fraction of (0.30$\pm$0.11)%. This number is in good agreement with the branching fraction of (0.25$\pm$0.10)% we obtain if we assume the marginal χ_{c2} signal is real.

The limit on the branching fraction for $B{\rightarrow}\eta_c$X of 0.9% is a factor of two to four above the expected theoretical branching fraction [3,32,33].

XI. SUMMARY

We have reported a number of improved measurements of B-meson decays to final states with charmonium mesons. In particular we find inclusive branching fractions of $(1.12\pm0.04\pm0.06)\%$ for $B\to J/\psi$X, $(0.34\pm0.04\pm0.03)\%$ for $B\to\psi'$X, and $(0.40\pm0.06\pm0.04)\%$ for $B\to\chi_{c1}$X. We also find some indication of the inclusive production of χ_{c2}. A thorough analysis of J/ψ momentum spectrum in B-meson decay has been presented, as have first measurements of the inclusive ψ' and χ_{c1} momentum spectra. We set an upper limit for $B\to\eta_c$X of 0.9% at the 90% confidence level.

ACKNOWLEDGMENTS

We would like to thank Mikhail Voloshin for useful discussions. We gratefully acknowledge the effort of the CESR staff in providing us with excellent luminosity and running conditions. J.P.A., J.R.P., and I.P.J.S. thank the NYI program of the NSF, G.E. thanks the Heisenberg Foundation, I.P.J.S. and T.S. thank the TNRLC, K.K.G., M.S., H.N.N., T.S., and H.Y. thank the OJI program of DOE, J.R.P. thanks the A.P. Sloan Foundation, S.M.S. thanks the Islamic Development Bank, and A.W. thanks the Alexander von Humboldt Stiftung for support. This work was supported by the National Science Foundation, the U.S. Dept. of Energy and the Natural Sciences and Engineering Research Council of Canada.

REFERENCES

[1] M.K. Gaillard, B.W. Lee, Phys. Rev. Lett. **33**, 108 (1974).

[2] G. Altarelli, L. Maiani, Phys. Lett. B **52**, 351 (1974).

[3] J.H. Kühn, S. Nussinov, and R. Rückl, Z. Physik C **5**, 117 (1980).

[4] G.T. Bodwin, E. Braaten, T.C. Yuan, and G.P. Lepage, Phys. Rev. D **46**, 3703 (1992).

[5] C. Albajar *et al.* (UA1 Collaboration), Phys. Lett. B **256**, 112 (1991).

[6] F. Abe *et al.* (CDF Collaboration), Phys. Rev. Lett. **68**, 3403 (1992); F. Abe *et al.* (CDF Collaboration), Phys. Rev. Lett. **69**, 3704 (1992).

[7] D. Jansen *et al.* (E789 Collaboration), submitted to Phys. Rev. Lett.

[8] P. Haas *et al.* (CLEO Collaboration), Phys. Rev Lett. **55**, 1248 (1985).

[9] H. Albrecht *et al.* (ARGUS Collaboration), Phys. Lett. B **199**, 451 (1987).

[10] H. Albrecht *et al.* (ARGUS Collaboration), Z. Phys. C **48**, 543 (1990).

[11] D. Bortoletto *et al.* (CLEO Collaboration), Phys. Rev. D **45**, 21 (1992).

[12] R. Poling (CLEO Collaboration), *Proceedings of the Joint Lepton-Photon Symposium and Europhysics Conference on High Energy Physics*, edited by S. Hegarty, K. Potter and E. Quercigh (World Scientific, Singapore, 1992).

[13] H. Albrecht *et al.* (ARGUS Collaboration), Phys. Lett. B **277**, 209 (1992).

[14] M.S. Alam *et al.* (CLEO Collaboration), Phys. Rev. D**50**, 43 (1994).

[15] J.P. Alexander *et al.* (CLEO Collaboration), Cornell University preprint CLNS-94-1291 (1994).

[16] Y. Kubota *et al.* (CLEO Collaboration), Nucl. Instrum. Meth. A **320**, 66–113 (1992).

[17] G. Fox and S. Wolfram, Phys. Rev. Lett. **23**, 1581 (1978).

[18] D. Coffman, in preparation (1994).

[19] L. Montanet *et al.* (Particle Data Group), Phys. Rev. D **50**, 1173 (1994).

[20] Skwarnicki T., Ph.D. Thesis, Institute for Nuclear Physics, Krakow 1986; DESY Internal Report, DESY F31-86-02 (1986).

[21] D. Coffman *et al.* (Mark III Collaboration), Phys. Rev. Lett. **68**, 282 (1992).

[22] J.E. Fast (E760 Collaboration), in *The Fermilab Meeting, DPF '92*, edited by C.H. Albright *et al.* (World Scientific, Singapore, 1993).

[23] T.L. Trueman, Phys. Rev. D **18**, 3423, (1978); N.P. Chang and C.A. Nelson, Phys. Rev. D **20**, 2923, (1979).

[24] O. Adriani *et al.* (L3 Collaboration), Phys. Lett. B **317**, 467 (1993).

[25] J.H. Kühn and R. Rückl, Phys. Lett. B **135**, 477 (1984); ERRATUM-ibid **258**, 499 (1991).

[26] M. Neubert, V. Rieckert, Q.P. Xu and B. Stech, in *Heavy Flavours*, edited by A. J. Buras and H. Lindner (World Scientific, Singapore, 1992).

[27] M. Bauer, B. Stech, and M. Wirbel, Z. Physik C **34**, 103 (1987).

[28] I. Bigi *et al.*, University of Minnesota preprint UMN-TH-1234/94, to appear in *B Decays*, 2^{nd} edition, edited by S. Stone (World Scientific, Singapore, 1994).

[29] T. DeGrand and D. Toussaint, Phys. Lett. B **89**, 256 (1980).

[30] P.H. Cox, S. Hovater, S.T. Jones, and L. Clavelli, Phys. Rev. D **32**, 1157 (1985); ERRATUM-ibid **33** 295 (1986).

[31] T. Browder, K. Honscheid and S. Playfer, Cornell University reprint CLNS 93/1261, to appear in *B Decays*, 2^{nd} edition, edited by S. Stone (World Scientific, Singapore, 1994).

[32] P.H. Cox, S. Hovater and S.T. Jones, Phys. Rev. D **33**, 1503 (1986).
[33] N.G. Deshpande and J. Trampetic, Oregon University preprint OITS-546, 1994.

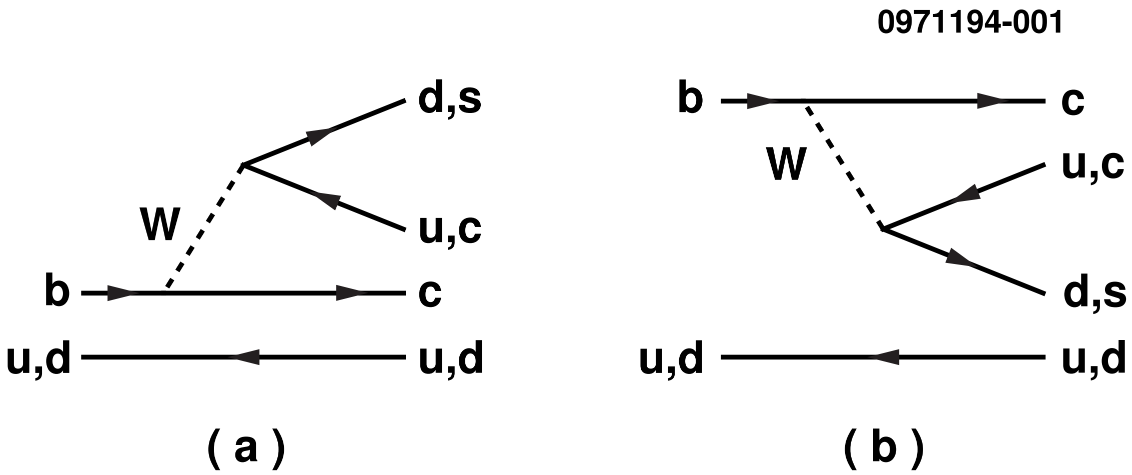

FIG. 1. Spectator diagrams for B-meson decays.

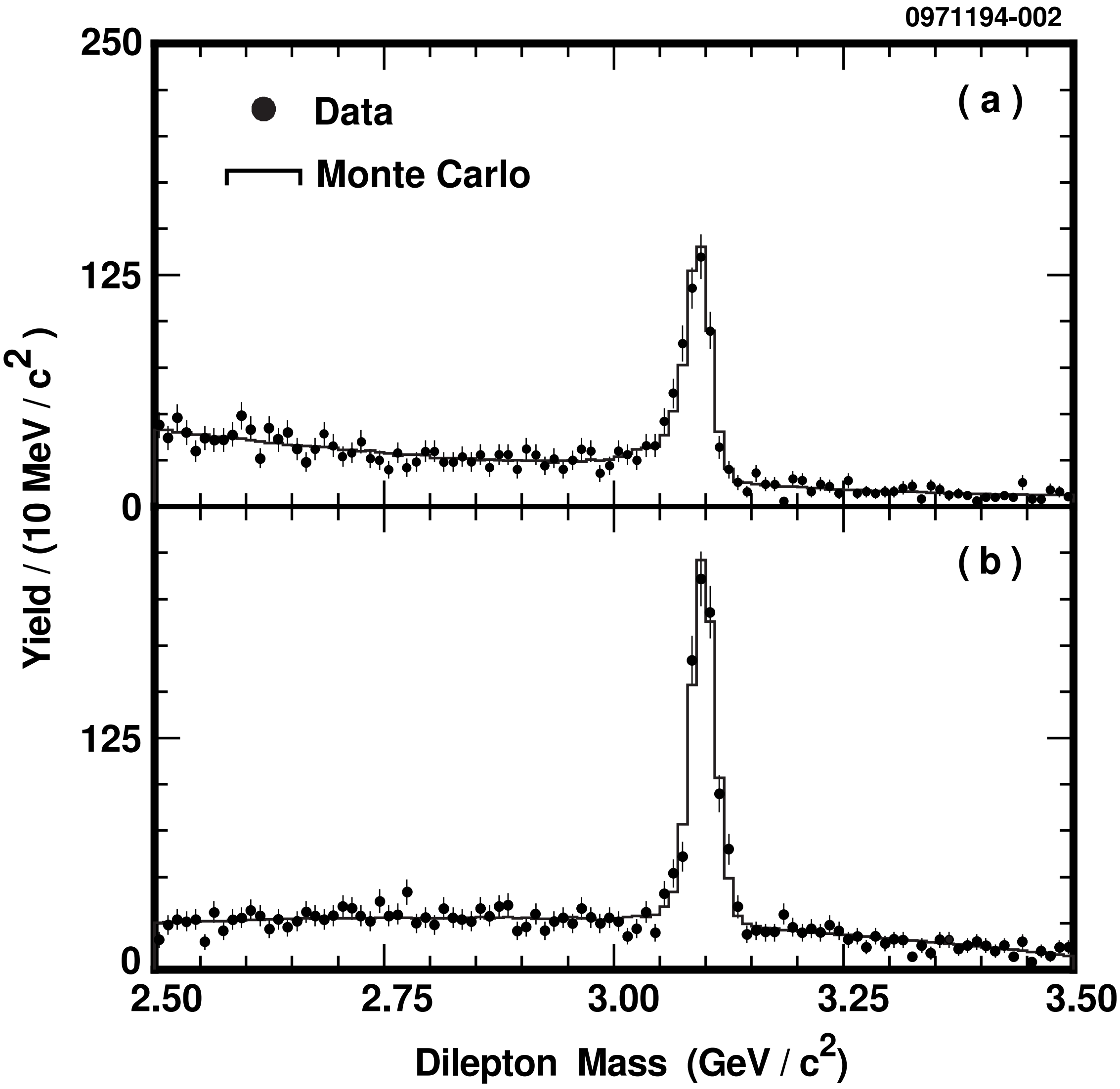

FIG. 2. Mass distributions for (a) dielectrons and (b) dimuons from B decays in CLEO-II $\Upsilon(4S)$ data. The fits are to Monte Carlo signal line shapes for $J/\psi \to \ell^+\ell^-$ and polynomial backgrounds.

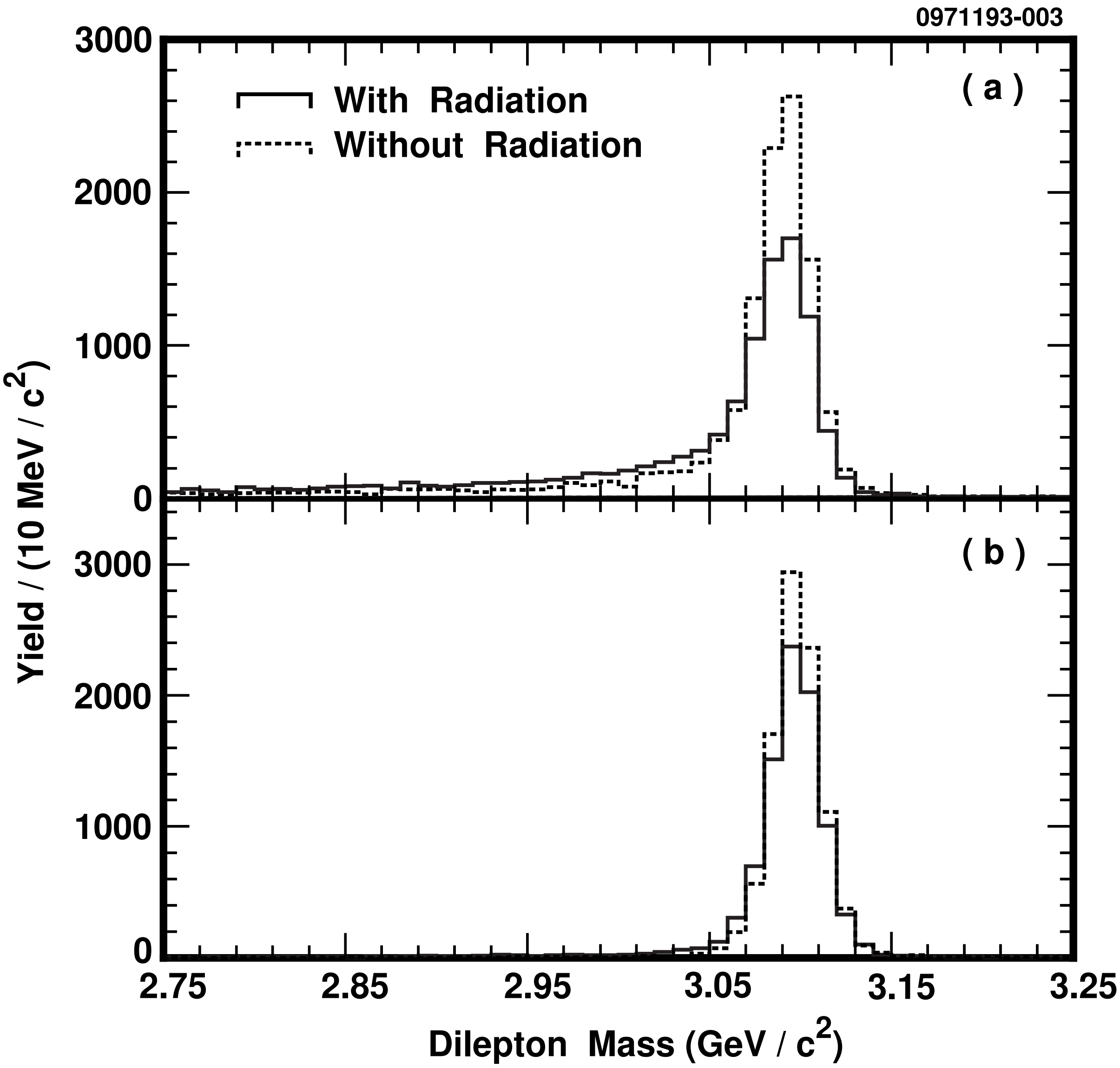

FIG. 3. Monte Carlo line shapes for (a) $J/\psi \to e^+e^-$ and (b) $J/\psi \to \mu^+\mu^-$ with and without final-state radiation. The effect of bremsstrahlung in detector material is included in all line shapes.

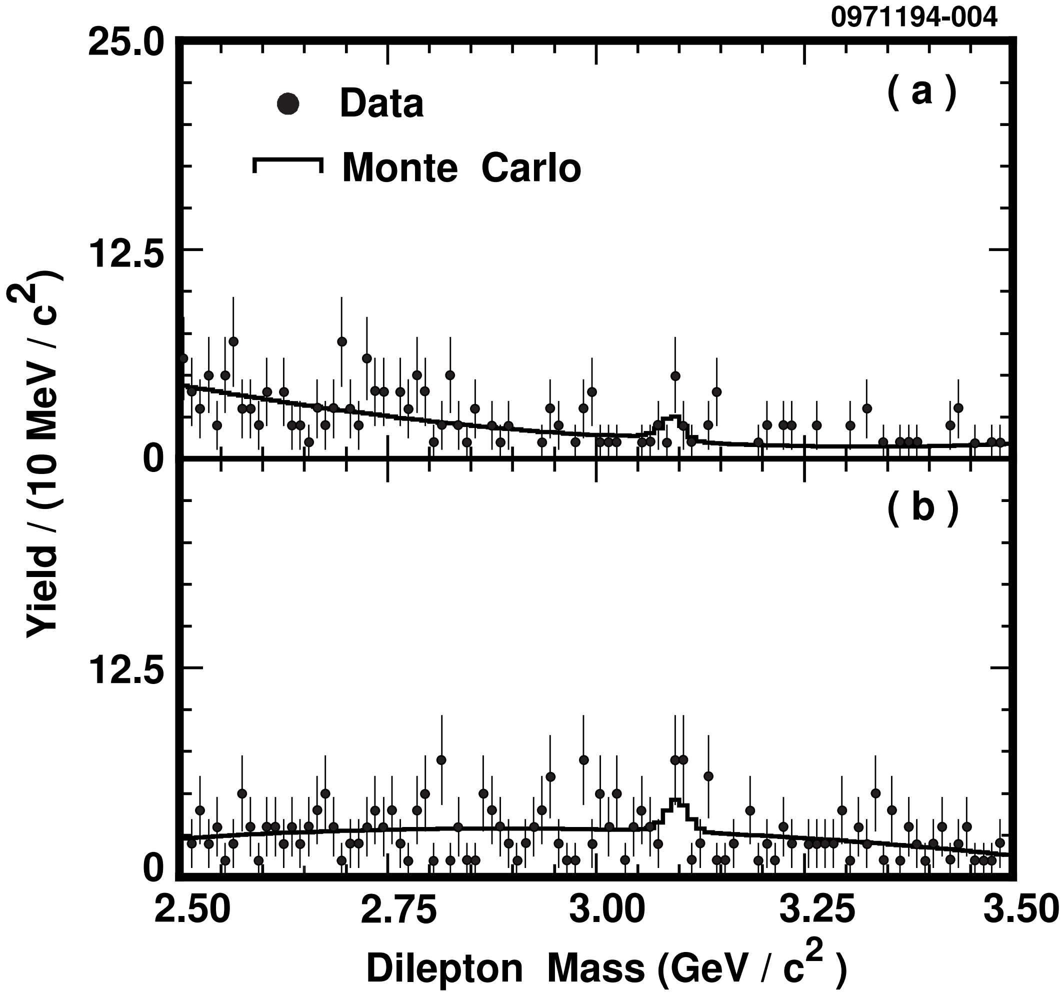

FIG. 4. Mass distributions from the continuum data sample for (a) dielectrons and (b) dimuons. The dilepton momentum was required to be be less than 2 GeV/c, and the Fox-Wolfram parameter R_2 was required to be less than 0.5. The fits are to Monte Carlo signal line shapes for $J/\psi \to \ell^+\ell^-$ and polynomial backgrounds.

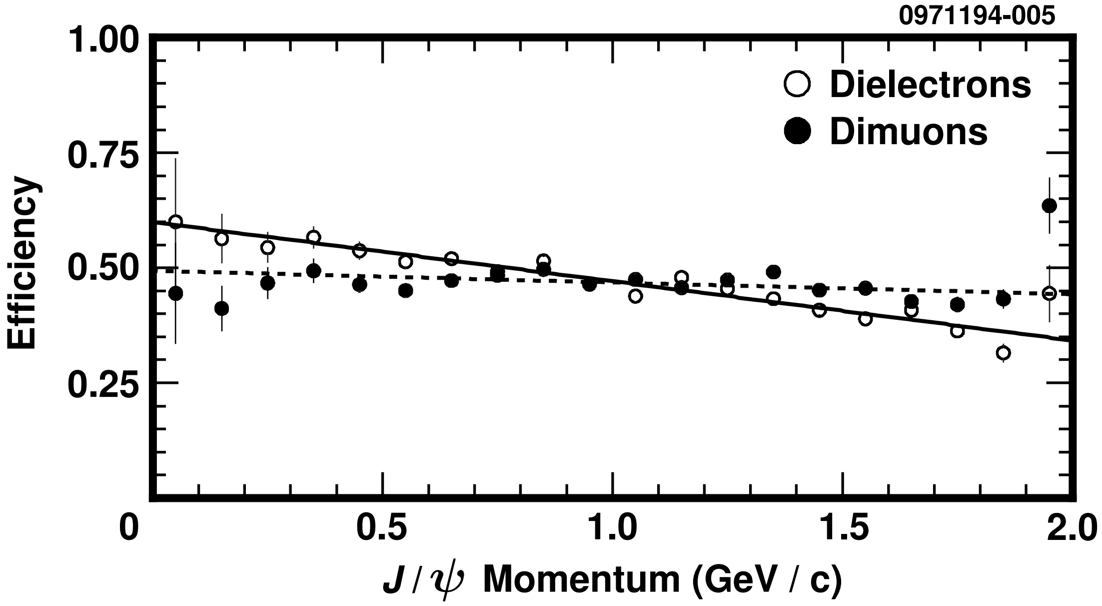

FIG. 5. Efficiency as a function of momentum for J/ψ's decaying to electrons and muons.

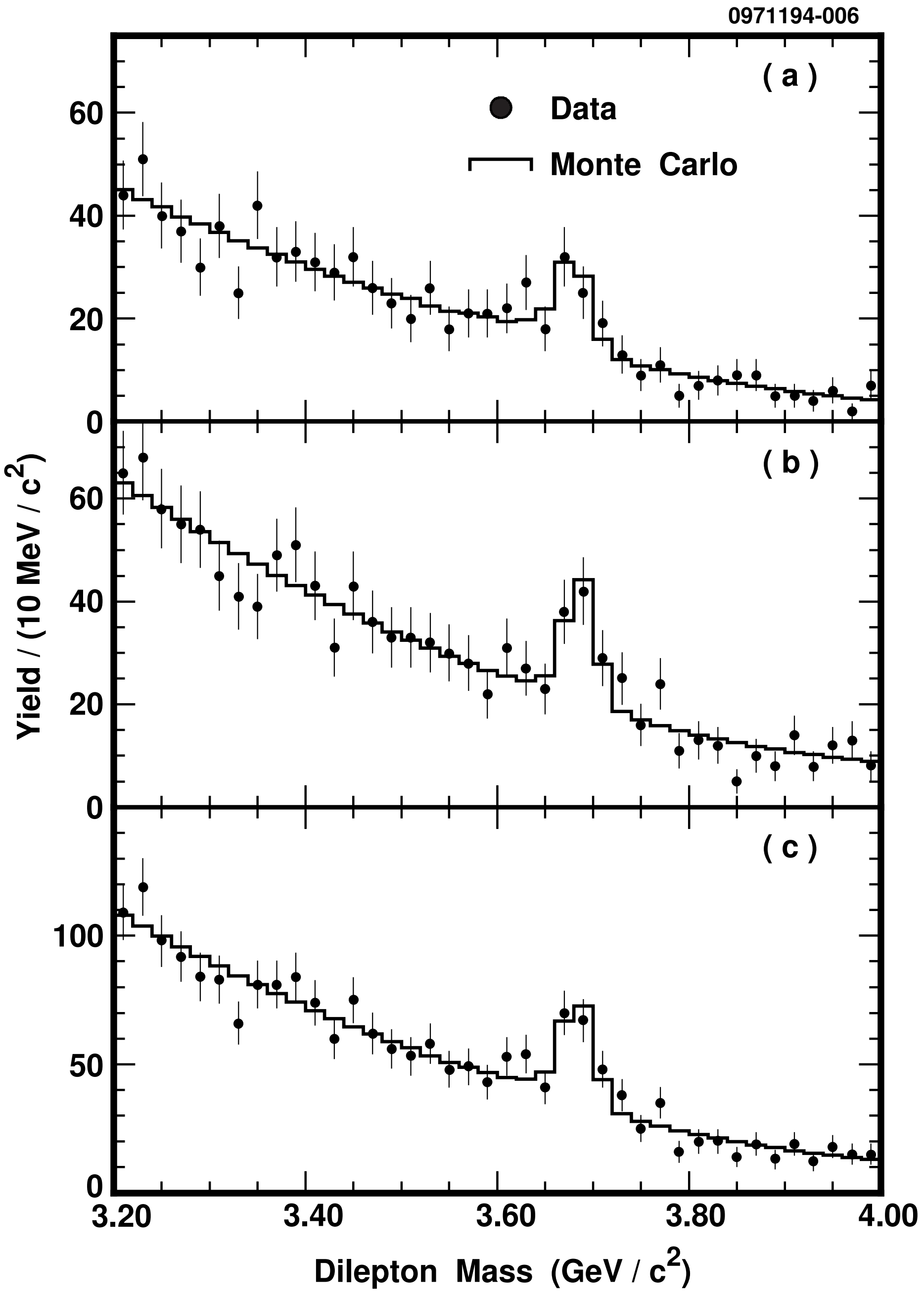

FIG. 6. Dilepton mass distributions for (a) dielectrons, (b) dimuons, and (c) the sum of dielectrons and dimuons. The fits are to a Monte Carlo signal line shape for the process $B \to \psi' X$, $\psi' \to e^+e^-$ or $\psi' \to \mu^+\mu^-$, and a polynomial background.

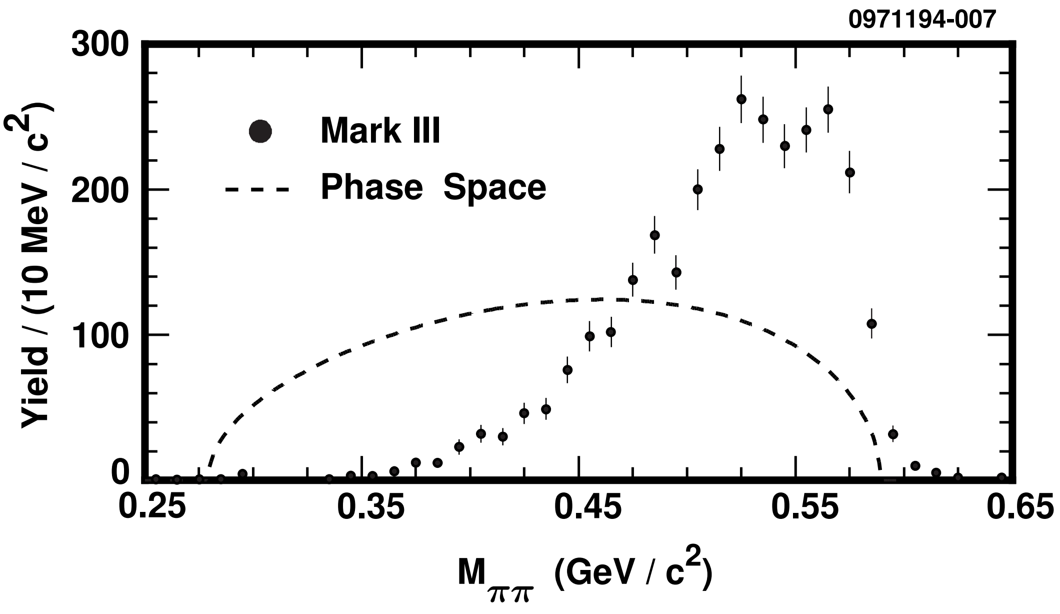

FIG. 7. The distribution of the the dipion mass for the decay $\psi' \to J/\psi \pi^+ \pi^-$. The dashed line shows the spectrum expected from phase space, while the points are the spectrum measured by Mark III[21].

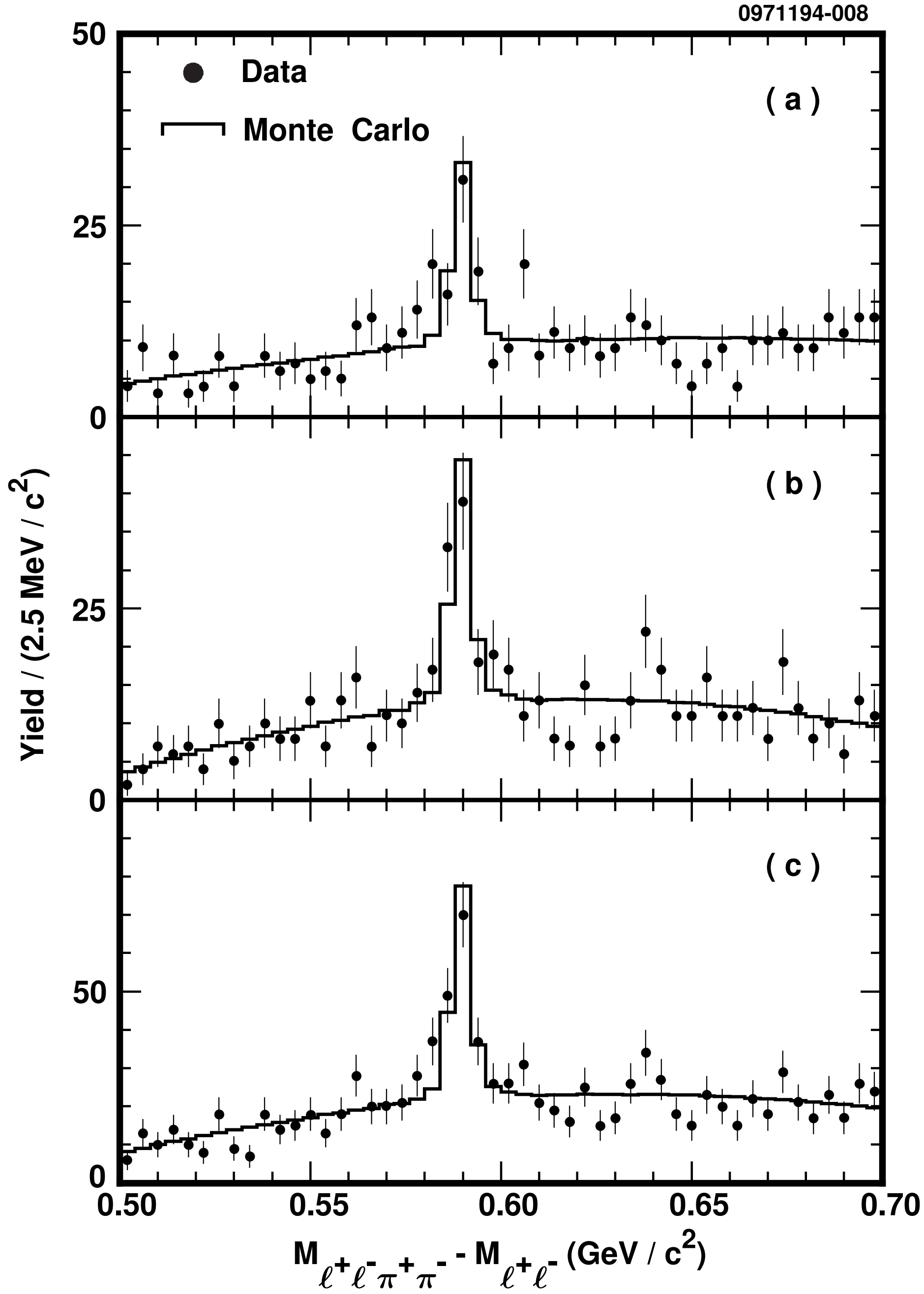

FIG. 8. Distributions of the difference between the $\ell^+\ell^-\pi^+\pi^-$ and $\ell^+\ell^-$ masses for (a) dielectrons, (b) dimuons, and (c) the sum of dielectrons and dimuons. The fit is to a Monte Carlo signal line shape for $\psi'\to J/\psi\pi^+\pi^-$ and a polynomial background.

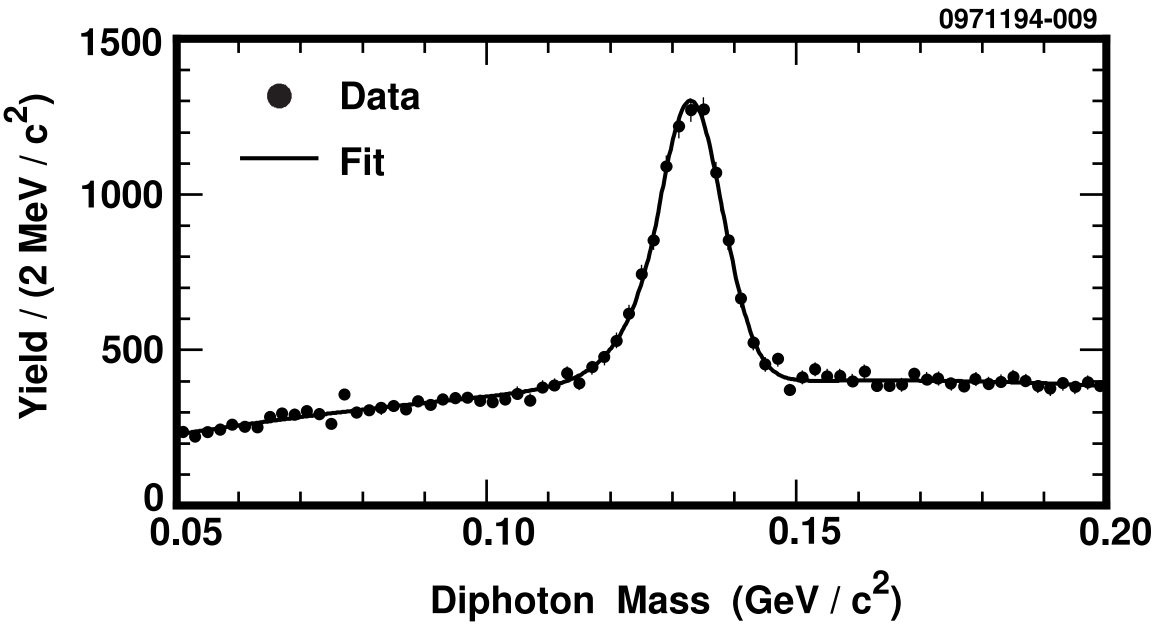

FIG. 9. Mass spectrum for diphotons with momenta between 0.4 and 0.8 GeV/c^2. Both photon candidates were required to be in the barrel region of the calorimeter. The fit to the signal is with the Crystal Ball function[20].

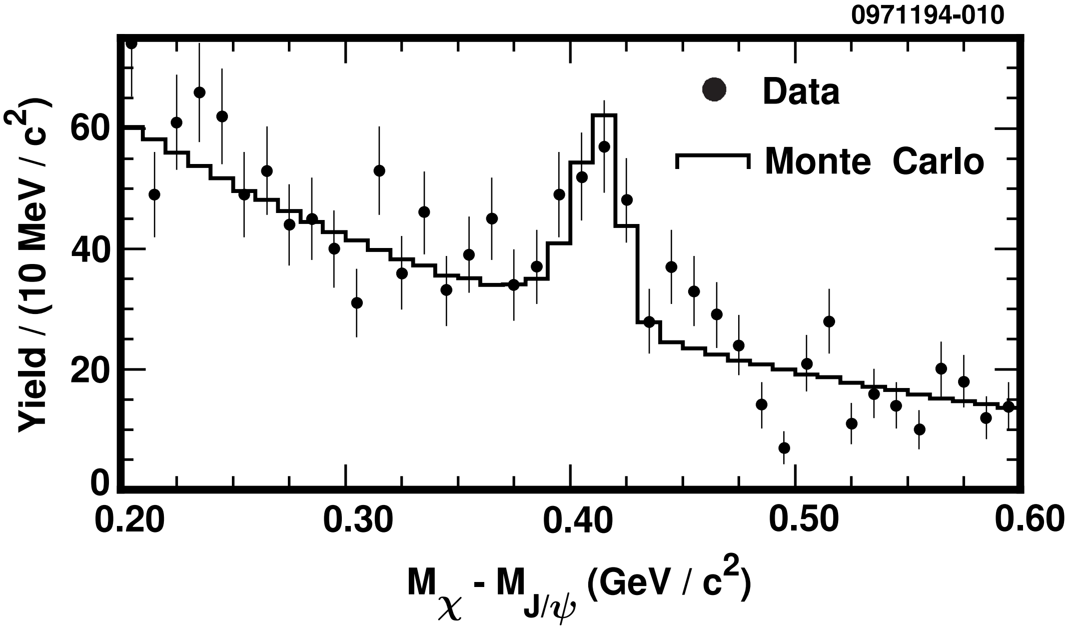

FIG. 10. Mass-difference distribution for $J/\psi\gamma$ candidates, with fit to $B\to\chi_{c1}$X Monte Carlo and polynomial background.

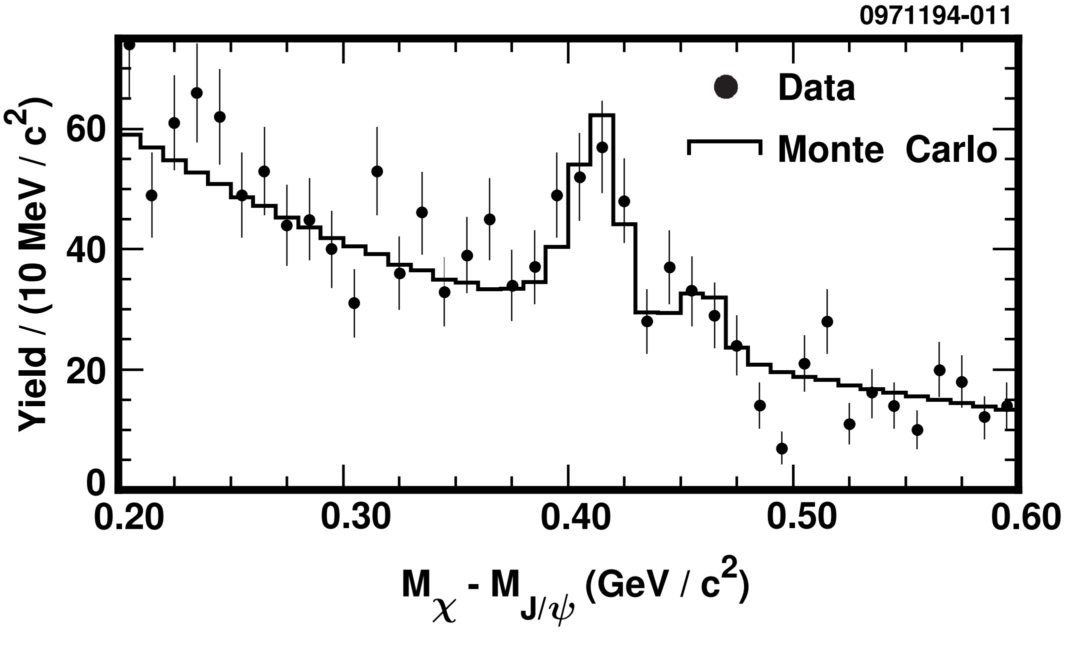

FIG. 11. Mass-difference distribution for $J/\psi\gamma$ candidates, with fit to $B\to\chi_{c1}$X and $B\to\chi_{c2}$X Monte Carlo and polynomial background.

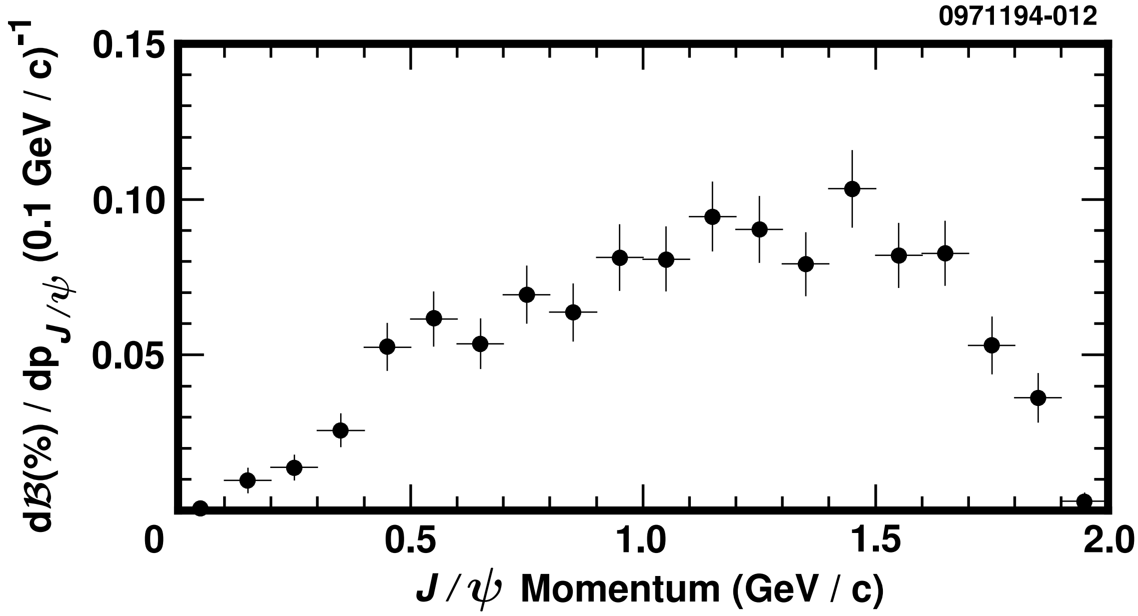

FIG. 12. Momentum spectrum for inclusive J/ψ production from B decays.

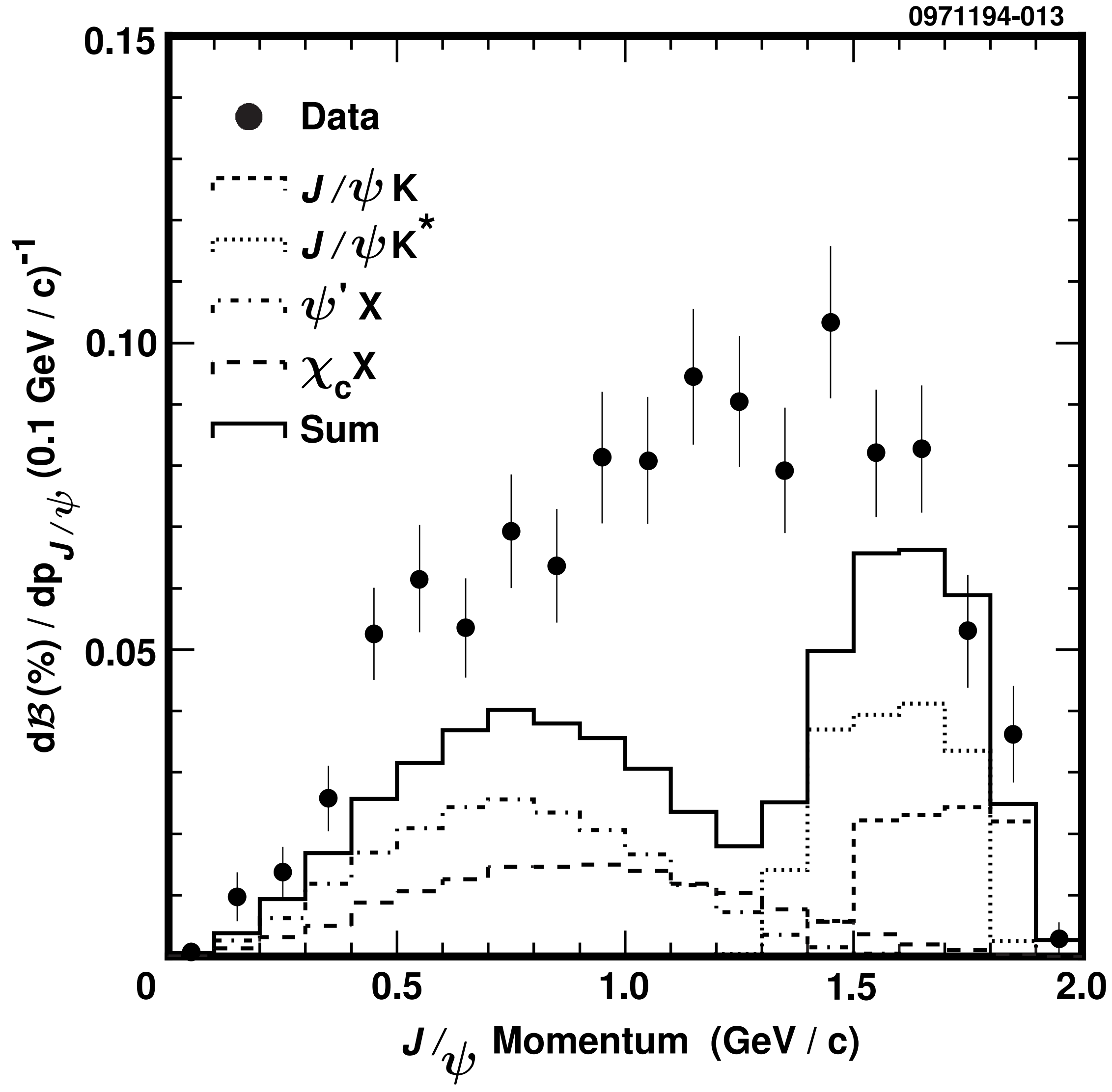

FIG. 13. Momentum spectrum for inclusive J/ψ production from B decays, overlaid with the expected momentum spectra for the exclusive processes $B \rightarrow J/\psi K$ and $B \rightarrow J/\psi K^*$, as well as the feed down from $B \rightarrow \psi' \mathrm{X}$ and $B \rightarrow \chi_c \mathrm{X}$.

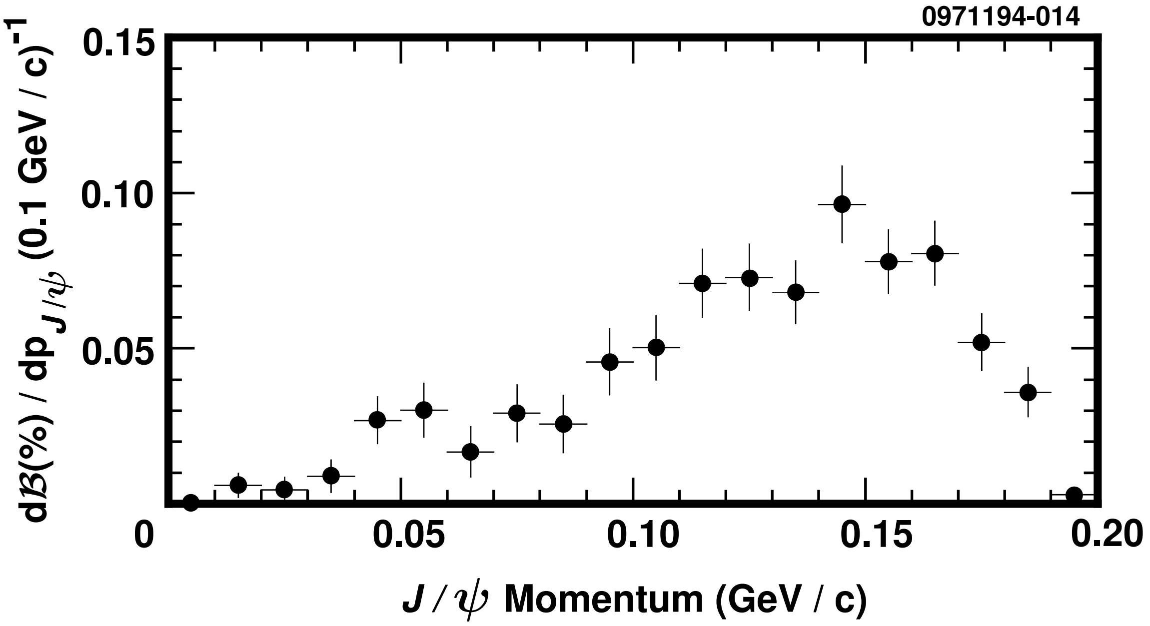

FIG. 14. Momentum spectrum for inclusive J/ψ production from B decays, with the expected contributions from $B \to \psi' X$, $\psi' \to J/\psi \pi^+ \pi^-$ and $B \to \chi_c X$, $\chi_c \to J/\psi \gamma$ subtracted.

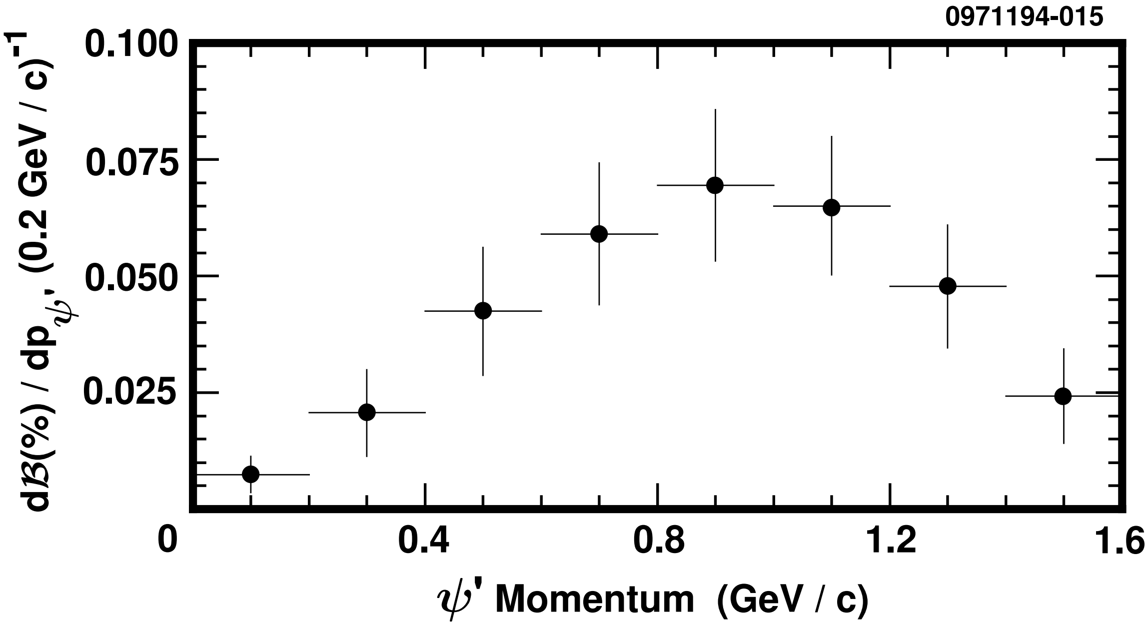

FIG. 15. Momentum spectrum for inclusive ψ' production from B decays.

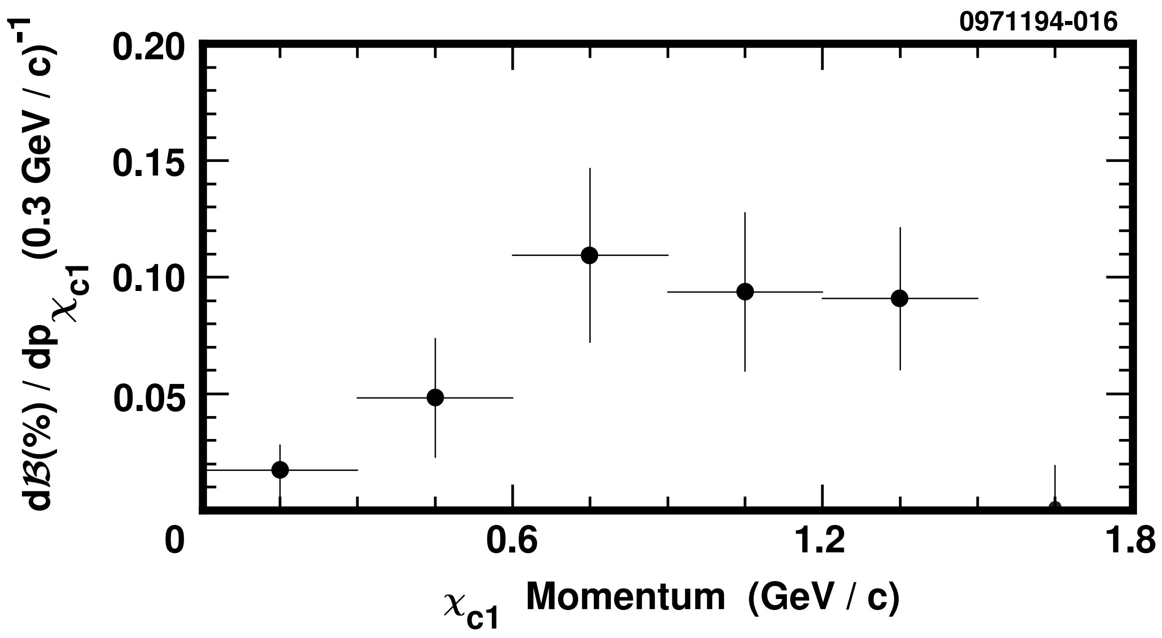

FIG. 16. Momentum spectrum for inclusive χ_{c1} production from B decays.

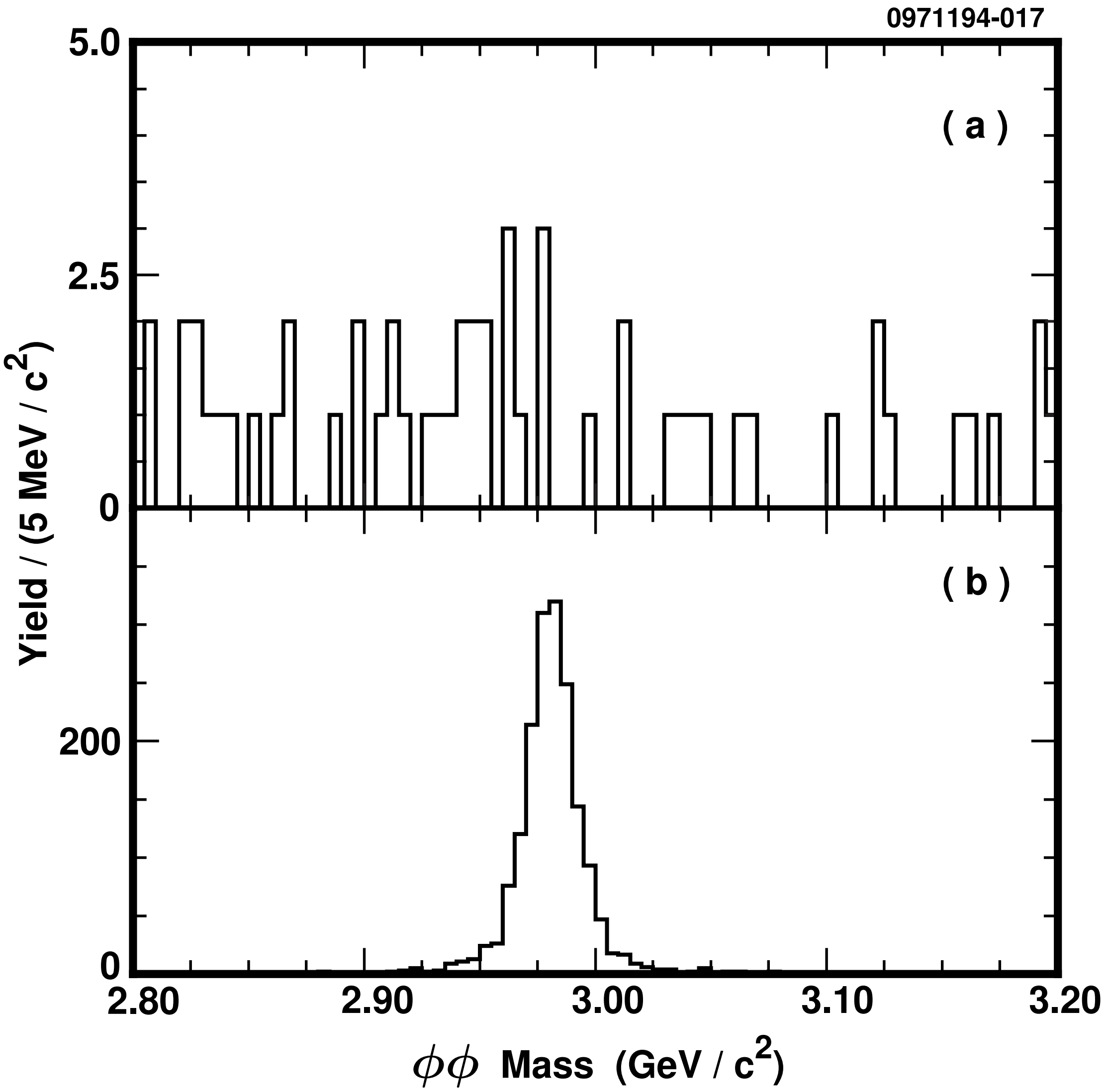

FIG. 17. Mass distributions for $\phi\phi$ candidates in (a) Υ(4S) data and (b) a Monte Carlo simulation of $B \to \eta_c$X.

TABLES

Uncorrelated	e^+e^-	$\mu^+\mu^-$
Branching fraction	4.2%	4.2%
Monte Carlo statistics	0.9%	0.9%
Monte Carlo momentum	2.0%	—
Monte Carlo line shape	1.0%	1.0%
Lepton ID	4.0%	4.7%
Total	6.3%	6.4%
Correlated		
Tracking	2.0%	
Number of B mesons	1.6%	
R_2 Distribution	2.0%	
Total	3.2%	

TABLE I. Contributions to the systematic uncertainty in the $B \to J/\psi X$ branching fraction measurement.

Charmonium	Yield	Branching Fraction (%)	PDG (%) [19]
η_c	<6.6	<0.9	
J/ψ	1455±52	1.12±0.04±0.06	1.30±0.17
$\psi' \to \ell^+\ell^-$	127±21	0.30±0.05±0.04	
$\psi' \to J/\psi\pi^+\pi^-$	113±16	0.37±0.05±0.05	
ψ' combined		0.34±0.04±0.03	0.46±0.20
χ_{c1}	112±17	0.40±0.06±0.04	
χ_{c2}	35± 13	<0.38	

TABLE II. Inclusive $B \to$Charmonium + X. For η_c and χ_{c2} the limits are at the 90% confidence level.

Decay Mode	Feed Down Mode	Feed Down BF (%) [19]	Measured BF (%)	Contribution to J/ψ(%)
$B \to J/\psi X$			1.12±0.04±0.06	1.12±0.07
$B \to \chi_{c1} X$	$\chi_{c1} \to J/\psi\gamma$	27.3±1.6	0.40±0.06±0.04	0.10±0.02
$B \to \chi_{c2} X$	$\chi_{c2} \to J/\psi\gamma$	13.5±1.1	0.25±0.10±0.03	0.03±0.01
$B \to \psi' X$	$\psi' \to J/\psi X$	57±4	0.34±0.04±0.03	0.19±0.03
$B \to J/\psi X$ (direct)				0.80±0.08
$B \to \chi_{c1} X$			0.40±0.06±0.04	0.40±0.07
$B \to \psi' X$	$\psi' \to \chi_{c1}\gamma$	8.7±0.8	0.34±0.04±0.03	0.03±0.01
$B \to \chi_{c1} X$ (direct)				0.37±0.07

TABLE III. Calculation of direct branching fractions for $B \to J/\psi X$ and $B \to \chi_{c1} X$.